Dissociative Attachment of Protons to 1-Fluoro- and 1-Chloroadamantane in the Gas Phase

J.-L. M. Abboud,*,† R. Notario,† E. Ballesteros,† M. Herreros,† O. Mó,‡ M. Yáñez,*,‡ J. Elguero,§ G. Boyer,⊥ and R. Claramunt⊥

Contribution from the Instituto de Química Física "Rocasolano", C.S.I.C., Serrano 119, E-28006 Madrid, Spain, Departamento deQuímica, C-14, Universidad Autónoma de Madrid, Cantoblanco, E-28049 Madrid, Spain, Instituto de Química Médica, C.S.I.C., Juan de la Cierva 3, E-28006 Madrid, Spain, and Departamento de Química Orgánica, UNED, Ciudad Universitaria, E-28040 Madrid, Spain

*Received August 25, 1993**

Abstract: An FTICR mass spectrometry study has shown that gas-phase protonation of 1-fluoro- and 1-chloroadamantane is followed by a carbon–halogen bond fission. This technique has also allowed the determination of the onset of these dissociative proton attachment reactions. The experimental findings are ratified by ab initio MO calculations showing that the equilibrium conformation of both protonated species correspond to an ion–dipole complex between the adamantyl cation and the corresponding hydrogen halide molecule. Both the theoretical and the experimental approaches indicate 1-fluoroadamantane to be more basic in the gas phase than 1-chloroadamantane. The structures and harmonic vibrational frequencies of the relevant species in these reactions are also examined.

1. Introduction

Cation association to organic molecules in the gas phase leads very often to significant bond activation effects. Particular attention was devoted to these phenomena when produced by atomic metal cations.[1-5] In this respect the review articles of Armentrout[6] and Watson[7] constitute good references regarding the state-of-the-art of this problem. However, these activations are not exclusive of interactions involving metal cations but may be significant also in gas-phase protonation processes.[8-11] On the other hand, ab initio calculations usually provide useful information on bond activation effects,[12-20] and quite often this information can assist the experimental work aimed at elucidating the mechanisms of intramolecular ion–molecule reactions and fragmentation pathways of metastable ions.

Consider a molecule R–X, in which R is an aliphatic or alicyclic group and X is a substituent endowed with lone pair electrons (F, Cl, OH, SH, NH_2). These species are known[21] to protonate in the gas phase, generally according to reaction 1:

$$R\text{–}X(g) + H^+(g) \rightarrow R\text{–}X\text{–}H^+(g) \qquad \Delta G^\circ_{(1)} \quad (1)$$

In some cases, reaction 1 is followed by reaction 2:

$$R\text{–}X\text{–}H^+(g) \rightarrow R^+(g) + XH(g) \qquad \Delta G^\circ_{(2)} \quad (2)$$

The overall process 3, a dissociative proton attachment (DPA), is well documented:[21a,22]

$$R\text{–}X(g) + H^+(g) \rightarrow R^+(g) + XH(g) \qquad \Delta G^\circ_{(3)} \quad (3)$$

Reactions 2 and 3 are favored by the thermodynamic stability of $R^+(g)$ and XH(g), as well as by a low intrinsic basicity of RX, GB(RX), defined as the negative of $\Delta G^0_{(1)}$.

In this work we seek to investigate some energetic and mechanistic characteristics of selected DPA reactions.[23]

On account of the above thermodynamic considerations and in view of our previous theoretical work on bond activation by

† Instituto de Química Física "Rocasolano".
‡ Universidad Autónoma de Madrid.
§ Institudo de Química Médica.
⊥ Ciudad Universitaria.

* Abstract published in *Advance ACS Abstracts*, February 15, 1994.

(1) Janowicz, A. H.; Bergman, R. G. *J. Am. Chem. Soc.* **1982**, *104*, 352.
(2) Hoyano, J. K.; Graham, W. A. G. *J. Am. Chem. Soc.* **1982**, *104*, 3723.
(3) Jones, W. D.; Feher, F. J. *J. Am. Chem. Soc.* **1982**, *104*, 4240.
(4) Janowicz, A. H.; Bergman, G. R. *J. Am. Chem. Soc.* **1983**, *105*, 3929.
(5) Hoyano, J. K.; McMaster, A. D.; Graham, W. A. G. *J. Am. Chem. Soc.* **1983**, *105*, 7190.
(6) Armentrout, P. B. In *Selective Hydrocarbon Activation: Principles and Progress*; Davies, J. A., Watson, P. L., Greenberg, A., Liebman, J. F., Eds.; VCH Publishers: New York, 1990; pp 467–533.
(7) Watson, P. L. In *Selective Hydrocarbon Activation: Principles and Progress*; Davies, J. A., Watson, P. L., Greenberg, A., Liebman, J. F., Eds.; VCH Publishers: New York, 1990; pp 79–112.
(8) Alcamí, M.; Mó, O.; Yáñez, M.; Abboud, J.-L.M.; Elguero, J. *Chem. Phys. Lett.* **1990**, *172*, 471.
(9) Esseffar, M.; El Mouhtadi, M.; López, V.; Yáñez, M. *J. Mol. Struct. (Theochem)* **1992**, *225*, 393.
(10) Abboud, J.-L.M.; Cañada, T.; Homan, H.; Notario, R.; Cativiela, C.; Díaz de Villegas, M. D.; Bordejé, M. C.; Mó, O.; Yáñez, M. *J. Am. Chem. Soc.* **1992**, *114*, 4728.
(11) Bordejé, M. C.; Mó, O.; Yáñez, M.; Herreros, M.; Abboud J.-L.M. *J. Am. Chem. Soc.* **1993**, *115*, 7389.
(12) Rappé, A. K.; Goddard, W. A., III *J. Am. Chem. Soc.* **1982**, *104*, 448
(13) Blomberg, M. R. A; Brandemark, U.; Siegbahn, P. E. M. *J. Am. Chem. Soc.* **1983**, *105*, 5557.
(14) Low, J. J.; Goddard, W. A., III *J. Am. Chem. Soc.* **1984**, *106*, 8321.
(15) Svensson, M.; Blomberg, M. R. A.; Siegbahn, P. E. M. *J. Am. Chem. Soc.* **1991**, *113*, 7076.
(16) Blomberg, M. R. A.; Siegbahn, P. E. M.; Svensson, M. *J. Am. Chem. Soc.* **1992**, *114*, 6095.
(17) Total, A.; Tortajada, J.; Morizur, J. P.; Alcamí, M.; Mó, O.; Yáñez, M. *J. Phys. Chem.* In press.
(18) Siegbahn, P. E. M.; Blomberg, R. A. *J. Am. Chem. Soc.* **1992**, *114*, 10548.
(19) Siegbahn, P. E. M.; Blomberg, M. R. A.; Svensson, M. *J. Phys. Chem.* **1993**, *97*, 2564.
(20) Mó, O.; Yáñez, M.; Total, A.; Tortajada, J.; Morizur, J. P. *J. Phys. Chem.* In press.
(21) (a) Uggerud, E. *Mass Spectrom. Rev.* **1992**, *11*, 389. (b) Aue, D. H.; Bowers, M. T. In *Gas Phase Ion Chemistry*; Bowers, M. T., Ed.; Academic Press: New York, 1979; Vol. 2, Chapter 9. (c) Lehman, T. A.; Bursey, M. M. *Ion Cyclotron Resonance Spectrometry*; Wiley-Interscience: New York, 1976; Chapter 3.
(22) (a) Jennings, K. R. In *Gas Phase Ion Chemistry*; Bowers, M. T., Ed.; Academic Press: New York, 1979; Vol. 2, Chapter 12. (b) Huntress, W. T., Jr.; Bowers, M. T. *Int. J. Mass Spectrom. Ion Phys.* **1973**, *12*, 1. (c) Bowers, M. T., Chesnavich, W. J.; Huntress, W. T., Jr. *Int. J. Mass Spectrom. Ion Phys.* **1973**, *12*, 357. (d) Gilbert, J. R.; van Koppen, P.; Huntress,W. T.; Bowers, M. T. *Chem. Phys. Lett.* **1981**, *82*, 455. (e) Theoretical aspects of DPAs are discussed in Nobes, R. H.; Radom, L. *Chem. Phys.* **1983**, *74*, 163.
(23) It should be mentioned that when this work was close to completion, a combined theoretical and experimental study on the unimolecular HF loss from protonated fluorobenzene was published (Hrusák, J.; Schröder, D.; Weiske, T.; Schwarz, H. *J. Am. Chem. Soc.* **1993**, *115*, 2015). The mechanism of this precess is completely different from those presented here.

0002-7863/94/1516-2486$04.50/0

protonation[8-11] or binding to metal cations in the gas phase,[17] it seemed to us that 1-fluoroadamantane (FAD) and 1-chloroadamantane (ClAD) were good candidates for these studies. Thus, it is known that alkyl fluorides and chlorides are feebly basic[24a] (as compared to homologous alcohols, thiols, and primary amines) while 1-adamantyl cation (AD^+), HF, and HCl are quite stable charged and neutral species, respectively.[24,25]

Because of the major structural changes following the protonation of FAD and ClAD, we have devoted particular attention to the harmonic vibrational frequencies and structures of the various species involved in these reactions. Relevance of the latter also follows from the fact that both solid FAD and solid ClAD present several phases (including plastic ones) at room temperature. This greatly hampers the accurate experimental determination of their structures.

2. Experimental Section

1-Fluoroadamantane. There are three different methods to prepare 1-fluoroadamantane: (i) starting from 1-adamantol,[26-29] (ii) starting from adamantane,[30] and (iii) starting from 1-bromoadamantane.[31] After several attempts, the third method was selected (it has been used also for the preparation of the sample used in the X-ray study[32]). Since 1-fluoroadamantane is very volatile, it was necessary to ensure that the temperature of the water bath during the evaporation of the solvent never exceeded 30 °C and to cool the trap with liquid nitrogen. With such precautions the yield of pure 1-fluoroadamantane reaches 80%, mp 225 °C (lit. mp 210–212 °C[31]). The ^1H and ^{13}C NMR spectra of our sample were identical with those already described.[31,33] The product gives correct analytical (C,H) and mass spectrometry results.

1-Chloroadamantane was purchased from Janssen Chimica (98% purity) and carefully purified by repeated sublimation.

DPA experiments were performed on a modified Bruker CMS-47 FT-ICR mass spectrometer, already used in previous studies.[34] The main modification was the insertion of a Balzers BVB 063H butterfly valve between the high-vacuum turbomlecular pump and the section containing the ion-trapping cell and the head of the Bayard-Alpert ionization gauge. Its high field strength easily allows reaction times in the 10^2-s range. MS/MS experiments were carried out using the standard Bruker software. Nominal XAD pressures were in the range 1–2 10^{-7} mbar. Pressures of B were 3 to 10 times larger, depending on the system. Ionization was achieved by electron impact and the nominal ionization energies were kept as low as possible, typically in the 9–13-eV range.

While the only results reported in Table 1 are those relevant to the discussion, we have examined the range of basicities of water–methylamine by steps of 1 kcal·mol^{-1} or less.

3. Computational Details

Since polarization effects are important when describing molecule–ion interactions, we have completely optimized the structure of fluoroadamantane (FAD) and chloroadamantane (ClAD) and their protonated species ($FADH^+$ and $ClADH^+$) at the 6–31G* level.[35] Although it can be argued that diffuse p components in the basis are also necessary to properly describe these interactions, the use of such bases for systems of this size becomes prohibitive and, on the other hand, for smaller molecules, we have shown[8] that the inclusion of diffuse components in the basis does not introduce any significant change on either the relative energetics or the topological features of the electronic charge densities and their Laplacians.

The harmonic vibrational frequencies were evaluated analytically and were used to characterize the minima of the potential energy surface, to evaluate the zero-point energy corrections to the corresponding protonation energies, and to investigate bond activation effects.

To account for the electronic correlation effects on the energetics of these species, and in particular on the value of the corresponding protonation energies, we have carried out single-point calculations using the Moller–Plesset perturbation theory[36] at second order (MP2) and employing the HF optimized structures. All these calculations have been carried out using the Gaussian-90 series of programs.[37]

Since the theoretical information on the structure and bonding characteristics of adamantane halogen derivatives is, as far as we know, lacking at least at the ab initio level, we have considered it of interest to analyze them in terms of the topological characteristics of the electronic charge density, ρ, and its Laplacian, $\nabla^2\rho$. These topological analyses are specially suited to describe bond activation or bond reinforcement phenomena. As we have shown recently,[8-11] bond activation in protonation processes can be detected by comparing the Laplacian of the charge densities of the protonated and neutral species. Actually, Bader et al.[38-40] have demonstrated that the Laplacian of the electronic charge density ($\nabla^2\rho$) identifies regions of space wherein ρ is locally concentrated ($\nabla^2\rho < 0$) or depleted ($\nabla^2\rho > 0$). Hence, bond activation should be accompanied by a decrease in the absolute value of $\nabla^2\rho$, while bond reinforcement would imply a more negative value of the Laplacian. Therefore, in general, an inspection of the topological characteristics of the Laplacian of the charge density will reveal the most significant charge redistributions undergone by the neutral upon H^+ association. On the other hand, the existence of a chemical bond implies the existence of a (3,–2) critical point in ρ, i.e., a point in which ρ presents two negative curvatures (λ_1,λ_2) and a positive one (λ_3), indicating that at that point the electronic charge density is minimum along the bond and maximum in the other directions. Usually the value of the density and its Laplacian at these points,

Table 1. Experimental Determination of the Onset of Reaction 4 for XAD Compounds

X	ref base (B)	$\Delta GB(B)^{a,b}$	$\Delta G°_{(3)}{}^{a,b}$
F	$(t\text{-}C_4H_9)_2CO$	−3.3[c]	−199.3 ± 2.0
	$CH_3COCH_2COCH_3$	−4.2[d]	
Cl	$CH_3CO(i\text{-}C_3H_7)$	+3.5[c]	−192.4 ± 2.0
	$CH_3O(t\text{-}C_4H_9)$	+2.4[d]	

[a] All values in kcal·mol^{-1}. [b] See ref 43. [c] DPA takes place. [d] DPA does not take place.

(24) (a) Lias, S. G.; Bartmess, J. E.; Liebman, J. F.; Holmes, J. L.; Levin, R. D.; Mallard, W. G. *J.Phys. Chem. Ref. Data* **1988**, *17*, Suppl. No. 1. Regarding the stability of AD^+(g), see, e. g.: (b) Kruppa, G. H.; Beauchamp, J. L. *J. Am. Chem. Soc.* **1986**, *108*, 2162. (c) Sharma, R. B.; Sen Sharma, D. K.; Hiraoka, K.; Kebarle, P. *J. Am. Chem. Soc.* **1985**, *13*, 3747. (d) Staley, R. H.; Wieting, R. D.; Beauchamp, J. L. *J. Am. Chem. Soc.* **1977**, *99*, 5964. Results of an ab initio, MP2–6-31G//6–31G study of AD^+ have recently been published: Dutler, R.; Rauk, A.; Sorensen, T. S.; Whitworth, S. M., *J. Am. Chem. Soc.* **1989**, *111*, 9024.

(25) *JANAF Thermochemical Tables*; U.S. Department of Commerce, NBS, 1965.

(26) Olah, G. A.; Nojima, M.; Kerekes,I. *Synthesis* **1973**, 786.

(27) Olah, G. A. *Synthesis*, **1974**, 653.

(28) Olah, G. A.; Welch, J. T.; Vankar, Y. D.; Nojima, M.; Kerekes, I.; Olah, J. A. *J. Org. Chem.* **1979**, *44*, 3872.

(29) Olah, G. A.; Watkins, M. *Organic Synthesis*; Wiley: New York, 1986; Collect Volume VI, p 628.

(30) Barton, D. H. R.; Hesse, R. H.; Markwell, R. E.; Pechet, M. M. *J. Am. Chem. Soc.* **1976**, *98*, 3034.

(31) Fort, R. C.; Schleyer, P. v. R. *J. Org. Chem.* **1965**, *30*, 789.

(32) Amoureux, J. P.; Bee, M.; Sauvajol, J. L. *Acta Crystallogr.* **1982**, *B38*, 1984. Amoureux, J. P.; Foulon, M. *Acta Crystallogr.* **1987**, *B43*, 470.

(33) Krishnamurty, V. V.; Iyer, P. S.; Olah, G. A. *J. Org. Chem.* **1983**, *48*, 3373.

(34) See, e.g.: Abboud, J. L. M.; Cabildo, P.; Cañada, T.; Catalán, J.; Claramunt, R. M.; de Paz, J. L. G.; Elguero, J.; Homan, H.; Notario, R.; Toiron, C.; Yranzo, G. I. *J. Org. Chem.* **1992**, *57*, 398. This paper also provides background references on FTICR.

(35) Hariharan, P. C.; Pople, J. A. *Theor. Chim. Acta* **1973**, *28*, 213.

(36) Pople, J. A.; Binkley, J. S.; Seeger, R. *Int. J. Quantum Chem. Symp.*, **1976**, *10*, 1.

(37) Gaussian 90, Revision I, Frisch, M. J.; Head-Gordon, M.; Trucks, G. W.; Foreman, J. B.; Schlegel, H. B.; Raghavachari, K.; Binkley, J. S.; Gonzalez, C.; Defrees, D. J.; Fox, D. J.; Whiteside, R. A.; Seeger, R.; Melius, C. F.; Baker, J.; Martin, R. L.; Kahn, L. R.; Stewart, J. J. P.; Topiol, S.; Pople, J. A., Gaussian Inc.: Pittsburgh PA, 1990.

(38) Bader, R. F. W.; MacDougall, P. J.; Lau, C. D. H. *J. Am. Chem. Soc.* **1984**, *106*, 1594.

(39) Wiberg, K. B.; Bader, R. F. W.; Lau, C. D. H. *J. Am. Chem. Soc.* **1987**, *109*, 985.

(40) Bader, R. F. W. *Atoms in Molecules. A Quantum Theory*; Oxford University Press: New York, 1990.

called bond critical points, permits the characterization of the bonding between two given atoms. In particular, the ratio between the two negative curvatures is a measure of the elipticity of the bond (defined as $\epsilon = 1 - \lambda_1/\lambda 2$), and hence a measure of the π character of the linkage. These topological calculations have been carried out using the AIMPAC series of programs.[41]

4. Results and Discussion

Let there be a gaseous mixture containing a 1-adamantyl halide (XAD, X = F, Cl) and a protonated base, BH^+.

The dissociative proton transfer from BH^+ to XAD, (reaction 4):

$$XAD(g) + BH^+(g) \rightarrow AD^+(g) + HX(g) + B(g) \quad (4)$$

will take place spontaneously for $\Delta G^0_{(4)} < 0$ (assuming a negigible dissociation barrier). It can be easily shown that $\Delta G^0_{(4)}$ is given by eq 4a:

$$\Delta G^\circ_{(4)} = \Delta G^\circ_{(3)} - \Delta G^\circ_{(5)} \quad (4a)$$

where $\Delta G^0_{(5)}$ pertains to reaction 5:

$$B(g) + H^+(g) \rightarrow BH^+(g) \quad (5)$$

In principle, an equilibrium should be experimentally observed when $\Delta G^0_{(3)} \approx \Delta G^0_{(5)} = -GB(B)$. Then, and because extensive sets of GB values are available,[24a] one should be in a position to determine $\Delta G^0_{(3)}$, that is, the ergonicity of the DPA reaction 3.

The experiments were carried using a high field strength FT-ICR mass spectrometer (details given in the Experimental Section). Mixtures of ADX and B were introduced into the high-vacuum section of the instrument and ionized by electron impact. Charged fragments (mostly from B) acted as primary proton sources. In general, after 1–2 s, the main ions present in the system were $BH^+(g)$ and $AD^+(g)$. The system was actually allowed to evolve for at least 5 s and then all ions with the exception of $BH^+(g)$ were swept off the ICR cell[42] by means of a radiofrequency ejection "chirp". Great care was taken in order to avoid the excitation of this ion and so use was made of the appropriate "ejection safety belt" in the ejection step. $BH^+(g)$ was then allowed to react for times of up to 100 s. During this period of time, the main reactions observed were first the formation of AD^+ and later on that of the hydrogen-bonded dimers of B, $B_2H^+(g)$, and (eventually) variable amounts of the $(AD–B)^+$ adduct. The formation of B_2H^+ at long reaction times is a familiar feature of proton-exchange studies. The formation of $AD–B^+$ is less so. It reflects both the electrophilicity of AD^+ and the stability of this ion with respect to proton loss.

In practice, given the experimental conditions of the ICR study, reaction 4 is essentially irreversible (the partial pressure of HX being extremely small). Thus, while a true equilibrium cannot be reached, the onset of reaction 4 can be clearly observed. Thus, by using bases of increasing GBs, the moment comes when starting from $BH^+(g)$, no $AD^+(g)$ can be observed. This onset is slightly blurred when close to the threshold of reaction 4 by the formation of minor amounts of $AD^+(g)$ from $BH^+(g)$ during the first few seconds of the second reaction period. Afterwards, the relative intensity of the signal does not increase significantly with time. This probably originates in minute amounts of non-thermalized $BH^+(g)$. While this effect fully disappears by slightly increasing the basicity of the reference base, we estimate that it introduces an uncertainty of approximately 1 kcal·mol^{-1}.

Furthermore, under the irreversible conditions of the experiments, reaction 4 may proceed even if $\Delta G^0_{(4)}$ is positive by 1 or perhaps 2 kcal·mol^{-1}. Thus, the observed thresholds are, strictly speaking, upper limits for the stability of XAD in the presence of BH^+.

The experimental results of our bracketing experiments are summarized in Table 1, wherein we indicate for each XAD the corresponding reference bases, B, their GBs referred to $NH_3(g)$, $\Delta GB(B)$,[43a] and the estimated value of $\Delta G^0_{(3)}$ (by taking $GB(NH_3) = 195.4$ kcal·mol^{-1}).[43b]

As we shall see in forthcoming sections, these experimental findings are described adequately by the ab initio theoretical description of the structural changes observed upon protonation and with the harmonic vibrational frequencies of both protonated species, the latter being of fundamental importance for a complete rationalization of these phenomena.

5. Geometries

We shall start our theoretical survey of the gas-phase protonation of FAD and ClAD by the analysis of the structural changes which take place in the processes. For this purpose, we shall first discuss the most outstanding geometrical features of both neutrals.

The optimized structures of FAD, ClAD, $FADH^+$, and $ClADH^+$ as well as that of adamantyl cation have been schematized in Figure 1. As we have mentioned in the Introduction, these compounds usually appear in different phases including in a glassy crystalline structure[44] which render the structure determination very difficult. Actually, the X-ray structure of FAD has been published[44] but the coordinates are neither in the papers nor in the CSD (Cambridge Structural Data Base, codename BICVOY). That of ClAD has also been determined by the same group in Lille[45] and the crystallographic coordinates are reported in the CSD (codename BILNOZ01). Due to the very complex nature of the disorder[46] the geometry is very distorted. Even an average of bond distances and bond angles to a C_{3v} point group leads to a geometry (see Figure 1) far from our optimized geometry, particularly for the bonds in which the substituted carbon atom participates.

According to our results, both derivatives, FAD and ClAD, present quite similar structures, indicating that the adamantyl moiety is not very sensitive to the kind of halogen substituent. The most significant changes affect the lengths of the bonds in which the substituted carbon atom (C1) participates. However, they are smaller than 0.01 Å. Similarly the corresponding bond angles subtended by the bonds which converge in C1 differ by less than 0.5°, while the remaining angles are almost identical. These structural characteristics are also reflected in the topological characteristics of the corresponding electronic charge densities. As shown in Table 2, the bonds of FAD and ClAD present identical characteristics, with practically identical values of the charge densities and their Laplacians at the bond critical points. Only for the bonds in which the C1 carbon atom participates, the charge densities for the fluorine derivative are slightly greater and the Laplacians slightly more negative than for the chlorine one, in agreement with the small structural differences mentioned above. This is likely due to the slightly different inductive effects associated to fluorine and chlorine substitution. Also interestingly, these single bonds present a non-zero elipticity (although quite small), which can be a consequence of the preferential accumu-

(41) AIMPAC programs package has been provided by J. Cheeseman and R. F. W. Bader.

(42) See, e.g.: Buchanan, M. V.; Comisarow, M. B. In *Fourier Transform Mass Spectrometry*; Buchanan, M. V., Ed.; ACS Symp. Ser. 359; American Chemical Society: Washington, DC, 1987; Chapter 1.

(43) (a) GB values for references used in this work originate in experimental data obtained in Prof. R. W. Taft's laboratory and reported in ref. 24a. They have been corrected by a factor of 1.068, as suggested by recent studies: Szulejko, J. E.; McMahon, T. B. *J. Am. Chem. Soc.* **1991**, *113*, 4448. (b) From the value of $PA(NH_3)$ as given by Smith and Radom (Smith, B. J.; Radom, L. *J. Am. Chem. Soc.* **1993**, *115*, 4885) and the entropy change for the protonation of NH_3 given in ref 24a.

(44) Amoureux, J. P.; Bee, M.; Sauvajol, J. L. *Acta Crystallogr.* **1982**, *B38*, 1984. Amoureux, J. P.; Foulon, M. *Acta Crystallogr.* **1987**, *B43*, 470.

(45) Foulon, M.; Belgrand, T.; Gors, C.; More, M. *Acta Crystallogr.* **1989**, *B45*, 404.

(46) A dynamic disorder as shown by ^{13}C NMR in the solid state, Huang, Y.; Gilson, D. F. R.; Butler, I. S.; Morin, F. *J. Phys. Chem.* **1991**, *95*, 2151.

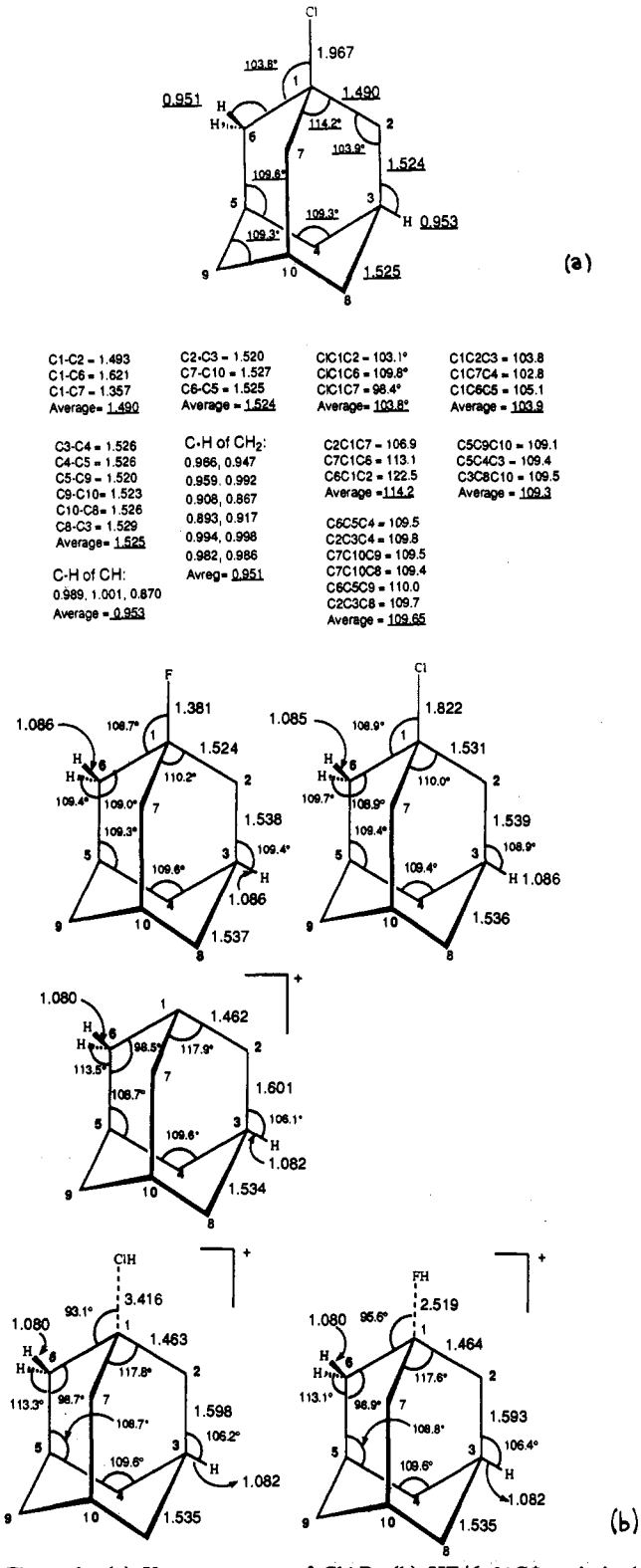

Figure 1. (a) X-ray structure of ClAD. (b) HF/6–31G* optimized structures of FAD, ClAD, AD^+, $FADH^+$, and $ClADH^+$. Bond lengths in angstroms and bond angles in degrees.

lation of charge density in the rings which converge on C1. In any case this effect is so small that it cannot account for any peculiarity of the adamantyl moiety.

The most dramatic changes take place upon protonation and corroborate the DPA observed experimentally, since, as illustrated in Figure 1, protonation leads to C–F and C–Cl bond cleavages of both FAD and ClAD. A comparison between the structures of both protonated species and that of adamantyl cation clearly indicates that the former correspond to ion–dipole complexes between this cation and the corresponding hydrogen halide molecules. This is also mirrored in the topological characteristics of both the C–F and C–Cl bonds, which in the protonated species present values of ρ and $\nabla^2\rho$ typical of ionic interactions. Also, the charge densities at the F–H and Cl–H bond critical points are almost identical with those in the corresponding diatomic molecules (see Table 2). The charge redistribution within the adamantyl moiety is also apparent. It can be observed that with respect to FAD and ClAD, the bonds in which the substituted carbon atom (C1) participates present much higher charge densities and more negative Laplacians. Coherently, the bonds strengthen and considerably shorten. Quite on the contrary the C2–C3 type of bonds become activated and they present smaller charge densities and less negative Laplacians and accordingly slightly greater bond lengths. Finally, the changes undergone for the remaining C–C bonds (of the C3–C4 type) are almost negligible, and they become slightly reinforced and shorter (see Figure 1 and Table 2). This can be explained in similar terms to those offered in ref 9. Gas-phase protonation implies a significant charge transfer from the base to the bare proton. When the basic site is a very electronegative atom, as fluorine or chlorine, it recovers part of the charge transferred to the proton by depopulating the bond which links the basic atom to the base. For FAD and ClAD, this depletion is so significant that the bond breaks apart, and the positive charge of the system localizes on the adamantyl moiety. The appearance of a positive charge initially located at C1 implies a significant enhancement of its electronegativity and hence a strong polarization of the electronic charge density of the system toward this atomic center. This results in a redistribution of part of this positive charge between the three carbon atoms directly bonded to C1 and in an increase of the charge densities at the corresponding bond critical points. The obvious consequence is then a smaller enhancement of the electronegativity of the three carbon atoms bonded to C1, which depopulate the other C–C bonds in which they participate, which accordingly become activated.

The increase in the electronegativity of C1 is also reflected in an increase of the *s* character of the hybrid orbitals centred at this atom, and hence in a dramatic increase of the corresponding bond angles (see Figure 1). As expected from the discussion above, the charge distribution of adamantyl cation is practically identical with that found for the protonated species of both FAD and ClAD.

6. Harmonic Vibrational Frequencies

Many of the structural features presented in the previous section are also reflected in the harmonic vibrational frequencies of these systems. To our knowledge, only the IR and Raman spectra of FAD have been published[47] and hence we have considered it of interest to compare our theoretical estimations with the experimental values and to present those of ClAD and the adamantyl cation, since they may guide some future experimental work on these systems. The harmonic vibrational frequencies for these three species, scaled by the empirical factor 0.89,[48] have been summarized in Table 3.

Since both FAD and ClAD belong to the C_{3v} point group, 7 of their normal modes are of a_2 symmetry and hence IR and Raman inactive. From the remaining active modes, 24 are degenerate since they belong to the *e* irreducible representation and 17 are a_1. Then, for the sake of conciseness, Table 3 presents only the frequency values of the 41 *e* and a_1 IR active modes.

Comparison between theoretical estimations and experimental values is not straightforward, because haloadamantanes exhibit one- and two-phase transitions to ordered phases. As a conse-

(47) Kawai, N. C.; Gilson, D. F. R.; Butler, I. S. *Can. J. Chem.* **1991**, *69*, 1758.

(48) Pople, J. A.; Krishnan, R.; Schlegel, H. B.; Binkley, J. S. *Int. J. Quantum Chem. Symp.* **1979**, *13*, 225.

Table 2. Bond Characteristics of FAD, ClAd, $FADH^+$, $ClADH^+$, and Adamantyl Cation

	C1–X10			C1–C2			C2–C3			C3–C4			X10–H	
compd	ρ^a	$\nabla^2\rho^b$	ϵ	ρ^a	$\nabla^2\rho^b$	ϵ	ρ^a	$\nabla^2\rho^b$	ϵ	ρ^a	$\nabla^2\rho^b$	ϵ	ρ^a	$\nabla^2\rho^b$
FAD	0.225	0.475	0.0	0.268	–0.743	0.05	0.252	–0.654	0.0	0.254	–0.662	0.0		
ClAD	0.170	–0.250	0.0	0.260	–0.700	0.02	0.252	–0.654	0.0	0.254	–0.664	0.0		
$FADH^+$	0.017	0.037		0.288	–0.886	0.07	0.213	–0.469	0.0	0.255	–0.668	0.0	0.339 (0.339)[c]	–2.935
$ClADH^+$	0.013	0.030		0.289	–0.888	0.07	0.212	–0.466	0.0	0.254	–0.670	0.0	0.221 (0.220)[d]	–3.555
adamantyl cation				0.289	–0.889	0.07	0.212	–0.468	0.02	0.256	–0.673	0.0		

[a] In e/au^3. [b] In e/au^5. [c] Values corresponding to the F–H bond in hydrogen fluoride. [d] Values corresponding to the Cl–H bond in hydrogen chloride.

Table 3. Harmonic Vibrational Frequencies (cm^{-1}) for FAD, ClAD, and Adamantyl Cation and Experimental Frequencies[a] of the 50 Bands Observed in the IR and Raman Spectra of Phase II of FAD

FAD		ClAD	adamantyl cation	FAD (exptl)		
				Raman[c]		IR
255(e)(dp)[b]	C–F bend	204(e)		264(dp)	266	
375(e)(dp)	C–C–C def + C–F bend	328(a_1)			391	
382(e)(dp)	C–C–C def	342(e)	316(e)(dp)		395	
403(a_1)(pp)	C–C–C def	386(e)	341(e)(dp)	420(pp)	420	419
447(e)(dp)	C–C–C def	434(e)	436(e)(dp)	465(dp)	467	463
525(a_1)(p)	C–C–C def	459(a_1)	438(a_1)(pp)	540(p)	539	538
626(e)(dp)	C–C–C def	627(e)	545(e)(dp)		643	641
696(a_1)(p)	cage breathing	663(a_1)	653(a_1)(p)		724	668
737(a_1)(p)	C–C st	730(a_1)	719(a_1)(p)	730(p)	731	729
777(e)(dp)	C–C st	776(e)	726(e)(dp)	774(p)	775	773
875(e)(dp)	CH_2 def	799(a_1)	750(a_1)(p)		814	814
900(e)(dp)	C–C st	871(e)	824(e)(dp)			904
905(a_1)(pp)	C–C st	900(e)	855(a_1)(dp)	920(pp)	918	918
957(a_1)(dp)	C–C + C–F st	933(a_1)	875(e)(dp)	931(dp)	935	933
961(e)(dp)	C–C st	957(e)	943(e)(dp)		959	968
1022(e)(dp)	C–C st	1012(a_1)	990(e)(dp)	970(dp)	970	970
1076(a_1)(dp)	C–C + C–F st	1025(e)	996(a_1)(dp)	988(dp)	990	
1092(e)(dp)	C–C st	1088(a_1)	1062(a_1)(dp)		1070	1045
1121(a_1)(dp)	C–F st + C–C–C bend	1093(e)	1066(e)(dp)	1076(dp) 1074		1072
1175(e)(dp)	CH_2 def	1178(e)	1117(e)(dp)		1080	1079
1267(e)(dp)	CH_2 def	1263(e)	1198(a_1)(p)	1102(dp) 1105		1105
1293(e)(dp)	C–C st	1294(e)	1205(e)(dp)			1113
1324(a_1)(dp)	C–C st + C–C–C bend	1318(a_1)	1262(e)(dp)			1184
1332(e)(dp)	C–C st	1327(e)	1311(a_1)(dp)	1180(dp) 1190		
1356(e)(dp)	CH_2 def	1357(e)	1321(e)(dp)		1195	
1372(a_1)(dp)	C–C–C bend	1365(a_1)	1355(e)(dp)	1265(dp) 1273		1268
1373(e)(dp)	C–C st	1372(e)	1364(e)(dp)			1295
1459(e)(dp)	CH_2 def	1458(e)	1450(e)(dp)		1302	1299
1471(e)(dp)	CH_2 def	1470(e)	1468(a_1)(p)			1316
1475(a_1)(p)	CH_2 def	1473(a_1)	1478(e)(dp)		1324	1322
1497(a_1)(p)	CH_2 def	1494(a_1)	1503(a_1)(p)			1346
2851(e)(dp)	C–H st	2851(e)	2877(e)(dp)			1354
2852(a_1)(pp)	C–H st	2852(a_1)	2881(a_1)(p)			1366
2862(e)(dp)	CH_2 st	2869(e)	2912(e)(dp)			1373
2868(a_1)(p)	CH_2 st	2874(a_1)	2914(e)(dp)	1439(dp)	1439	
2879(e)(dp)	CH_2 st	2881(e)	2918(a_1)(dp)			1449
2880(e)(dp)	CH_2 st	2882(e)	2921(a_1)(dp)			1456
2888(a_1)(dp)	CH_2 st	2890(a_1)	2926(e)(dp)	2851(p)	2852	2851
2889(a_1)(p)	CH_2 st	2891(a_1)	2928(a_1)(p)	2857(pp)	2858	2857
2894(a_1)(dp)	CH_2 st	2909(a_1)	2971(a_1)(dp)	2864(dp)	2863	2862
2903(e)	CH_2 st	2916(e)	2977(e)(dp)	2901 2909	2896	2891 2911 2917
				2925(p) 2931		2930
				2958(p) 2959	2938	

[a] Taken from ref 47. [b] dp, pp, and p stand for depolarized, partially polarized, and polarized, respectively. [c] The first column corresponds to the Raman spectrum obtained in CS_2 solution at 295 K. The second column corresponds to the Raman spectrum of phase II.

quence of this general behavior, a total of 50 bands have been observed in the IR and Raman spectra of phase II of FAD.[47] Nevertheless, there is a good agreement between our calculated frequencies and the experimental ones for CCF bending modes, cage deformations, C–C stretchings, CH_2 deformations and C-H stretchings. Also, in agreement with experimental evidence, our results indicate that seven a_1 bands are polarized. However, while Kawai et al., assign a band at 730 cm^{-1} to the C–F stretching

Table 4. Total Energies (hartrees), Zero-Point Energies (ZPE) (kcal·mol^{-1}), Total Entropy Values (S) (cal·mol^{-1}·K^{-1}), and Proton Affinities (PA) (kcal·mol^{-1}) for Relevant Species

species	HF/6-31G*	ZPE	S	MP2/6-31G*//6-31G*	PA[a]
FAD	−486.87782	158.7	83.4	−488.36195	184.2
ClAD	−846.93583	157.8	86.0	−848.37623	177.7
$FADH^+$	−487.19691	162.7	101.1	−488.66135	
$ClADH^+$	−847.24536	160.8	108.5	−848.66367	
AD^+	−387.18030	155.7	80.3	−388.46477	

[a] MP2 values with ZPE corrections included.

displacement, our ab initio calculations indicate that the a_1 band which presents the largest C–F stretching character appears at much higher frequency (1121 cm^{-1}). In this respect, it must be indicated that, in general, carbon–fluorine stretching vibrations usually show[49] strong absorptions in the region 1100–1300 cm^{-1}, in agreement with our results. Our treatment also predicts similar IR spectra for FAD and ClAD, as should be expected from the strong similarity between their structures. There are small differences regarding the C–Cl and C–F bending modes,and also regarding the C–F and C–Cl stretching frequencies. For ClAD, the latter appear at lower frequencies (799 cm^{-1}), explaining the different order predicted for the a_1 bands in the 700–1100 cm^{-1} region for both compounds.

Adamantyl cation presents three vibrational modes less than FAD and ClAD, which correspond to the e bending mode of the C1–halogen bond of the neutrals and to the a_1 C1–halogen stretching vibration. In general, as should be expected, the C–C stretching modes of the cation appear shifted to slightly lower frequencies than for the neutral halogen derivatives, while the C–H stretching displacements are slightly shifted to higher frequency values.

Also, the harmonic vibrational frequencies of the protonated species are consistent with the experimentally observed DPA. From the 75 vibrational frequencies of the protonated forms of both FAD and ClAD, 69 are practically identical with those of adamantyl cation. The strong bands predicted at 3819 cm^{-1} for $FADH^+$ and at 2829 cm^{-1} for $ClADH^+$ have frequencies extremely close to those of HF (3892 cm^{-1}) and HCl (2847 cm^{-1}) neutral molecules, respectively. The remaining 5 vibrational modes correspond to the bendings of the FH and ClH groups with respect to the adamantyl moiety and to a very loose C1–F and C1–Cl stretching, thus confirming that these protonated species correspond actually to an ion–dipole complex between the hydrogen halide molecule and the adamantyl cation.

7. Energetics of the DPA Processes

The total energies of the species under consideration are presented in Table 4. This table also contains the corresponding ZPEs as well as the values of the entropy terms. It must be noticed that our MP2 results predict FAD to be about 6 kcal·mol^{-1} more basic than ClAD in fairly good agreement with our experimental measurements. However, at the Hartree–Fock level both species are predicted to have the same basicity. This is a clear indication of the significant influence of correlation effects in the description of halogen bonds. This can be clearly illustrated by studying the relative stability of the neutrals. Combining eqs 6 and 7, eq 8 obtains which provides such information:

$$FAD(g) + H^+(g) \rightarrow AD^+(g) + HF(g) \quad (6)$$

$$AD^+(g) + HCl(g) \rightarrow ClAD(g) + H^+(g) \quad (7)$$

$$FAD(g) + HCl(g) \rightarrow HF(g) + ClAD(g) \quad (8)$$

From the experimental data in Table 1 it follows that $\Delta G^0_{(8)} = -6.4$ kcal·mol^{-1}. Using the ab initio MP2 values presented in Table 4 we calculate $\Delta G^0_{(8)} = -2.9$ kcal·mol^{-1}, while at the Hartree–Fock level the process is predicted to have a positive $\Delta G^0_{(8)} = +4.0$ kcal·mol^{-1}, contrary to experimental evidence.

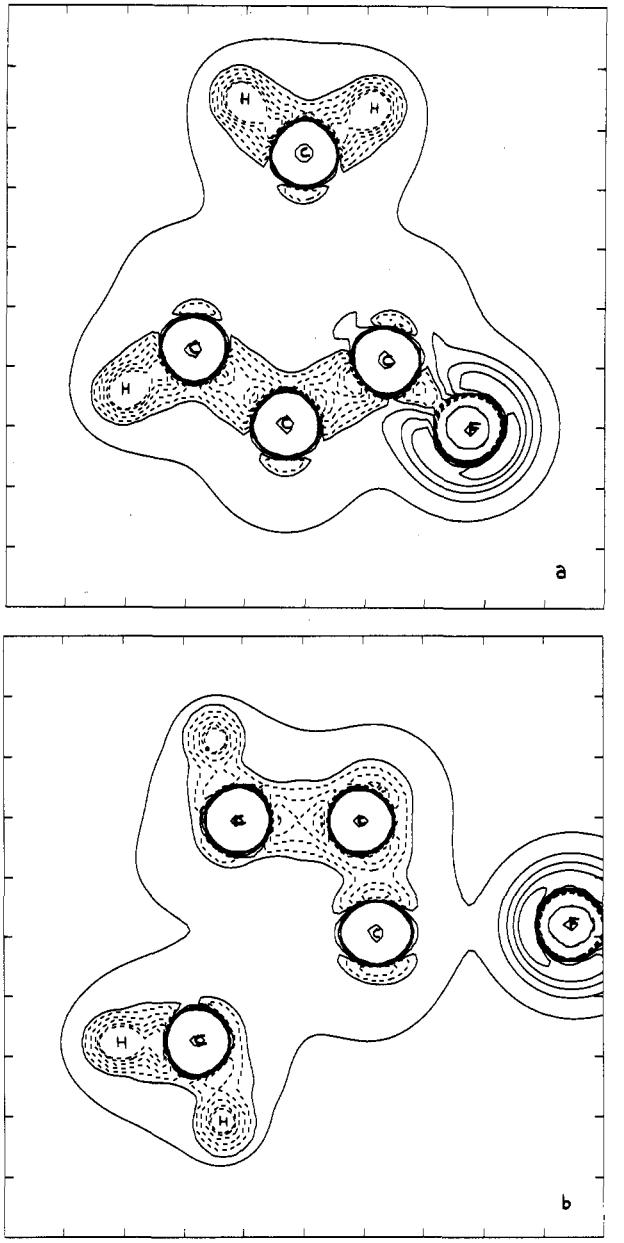

Figure 2. Contour map of the Laplacian of the charge density of (a) FAD, (b) $FADH^+$, evaluated in one of the symmetry planes containing the halogen atom, showing that gas-phase protonation of FAD is a clear DPA process. Positive values of $\nabla^2\rho$ are denoted by full lines and negative values by dashed lines. Contour values are ±0.05, ±0.25, ±0.50, ±0.75, and ±0.95 au.

Quite interestingly, in agreement with our previous conclusions regarding gas-phase protonation of alcohols and fluoroalkane,[9] there is a relationship between the calculated proton affinities of FAD and ClAD and the decrease in the charge density within the C–F and C–Cl bonds (see Table 2), which is larger in the former than in the latter.

The energetics of both protonated forms corroborates that they can be described as ion–dipole complexes between a singlet adamantyl cation and a hydrogen halide molecule. Actually, we have found that the complex formed by adamantyl cation, in its equilibrium conformation, and a hydrogen chloride molecule located the same distance from the former as in the $ClADH^+$ system has a total energy which differs from that of $ClADH^+$ by less than 0.06 kcal·mol^{-1}.

(49) Hudlicky, M. *Organic Fluorine Chemistry*; Plenum Press: New York. 1971.

In agreement with this, the contour maps of the Laplacians of the charge density of $FADH^+$ (see Figure 2) show that $\nabla^2\rho$ is clearly positive between the adamantyl moiety and the hydrogen halide molecule, as should be expected for an electrostatic interaction between two closed shell systems. Similar results obtain for $ClADH^+$.

The PAs reported in Table 4 are $-\Delta H^\circ$ values for reaction 9:

$$XAD(g) + H^+(g) \rightarrow XADH^+(g) \quad (9)$$

It is an experimental fact, however, that the adducts $ADXH^+(g)$ are never observed, $AD^+(g)$ being the only charged product. The reason for this behavior is as follows: As indicated above, these adducts are relatively loose ion–dipole complexes. ΔH° values (including ZPE and thermal corrections for reactions 10 and 11) amount respectively to 7.9 and 2.6 kcal·mol^{-1}.

$$FADH^+(g) \rightarrow AD^+(g) + HF(g) \quad (10)$$

$$ClADH^+(g) \rightarrow AD^+(g) + HCl(g) \quad (11)$$

Under the nominal working temperature of 333 K the $T\Delta S$ terms amount to 6.9 and 5.4 kcal·mol^{-1} respectively, from which we derive $\Delta G^0_{(10)} = +1.0$ kcal·mol^{-1} and $\Delta G^0_{(11)} = -2.8$ kcal·mol^{-1}. These standard Gibbs energy changes are in fact upper limits, because basis set superposition errors tend to make these values too positive by about 1 kcal·mol^{-1}. Hence, under the conditions of temperature prevailing in the ICR experiments, the spontaneous dissociation of $ClADH^+(g)$ is strongly favored. The dissociation of $FADH^+(g)$ is somewhat less so, but it is also driven to completion in the absence of significant amounts of HF(g).

8. Conclusions

Gas-phase protonation of 1-fluoro- and 1-chloroadamantane leads to carbon–halogen bond fission and hence to the formation of the very stable adamantyl cation. Both experimental and theoretical approaches show FAD to be more basic than ClAD. An onset of the DPA can be experimentally determined for both FAD and ClAD, and anticipating results to be published shortly, we can say that ab initio calculations confirm its existence.

Acknowledgment. This work has been partially supported by the Dirección General de Investigación Científica y Técnica, Projects PB90–0228-C02 and PL87–0357. Work by E.B. and M.H. was supported by a grant from Consejo Superior de Investigaciones Científicas.